On Localization Uncertainty in an Autonomous Inspection

Jan Faigl, Tomáš Krajník, Vojtěch Vonásek, Libor Přeučil

Abstract— **This paper presents a multi-goal path planning framework based on a self-organizing map algorithm and a model of the navigation describing evolution of the localization error. The framework combines finding a sequence of goals' visits with a goal-to-goal path planning considering localization uncertainty. The approach is able to deal with local properties of the environment such as expected visible landmarks usable for the navigation. The local properties affect the performance of the navigation, and therefore, the framework can take the full advantage of the local information together with the global sequence of the goals' visits to find a path improving the autonomous navigation. Experimental results in real outdoor and indoor environments indicate that the framework provides paths that effectively decreases the localization uncertainty; thus, increases the reliability of the autonomous goals' visits.**

I. Introduction

This paper concerns a problem of finding a reliable path for an autonomous mobile robot in the inspection task, i.e., a problem of finding a path to visit a set of goals. Having a model of the robot's workspace the required mission objective is to maximize the frequency of the goals' visits, which leads to minimize the inspection path length. However, due to a localization uncertainty, the path length is not the only criterion, and a precision of navigation is also considered during the path planning. The proposed approach follows the basic idea of the planning approaches considering robot position uncertainty that is to design a sequence of robot's actions to fulfill the desired mission objective while minimizing the position uncertainty. Let us briefly review previous approaches in this field.

The motion planning problem with uncertainty has been addressed using the "Sensory Uncertainty Field" notion in [1]. The approach provides estimation of possible errors in robot position computed by the localization function for every possible robot configuration. Then, a combination of the expected error with the path length is minimized during the path planning. In [2], authors formulate a problem of bearing-only target localization as an optimization problem of finding an optimal observer trajectory. Their approach is based on the Fisher information matrix (FIM) representing information contained in a sequence of measurements.

Authors of [3] proposed a path planning algorithm that finds a safe path in an uncertain-configuration space using a localization function based on the Kalman filter technique (EKF). Safe paths are also studied in [4], where authors address the problem of computationally intractable stochastic control problem as a path planning problem in a Bayesian framework using extended planning space that is created as a Cartesian product of robot poses and covariances. A safe path is determined by a state space searching algorithm, which finds a path as a sequence of state transitions using FIM. Although the approach is well formalized, the authors noted it is computationally demanding if states in the open list cannot be easy discarded due to a dominated state, i.e., the case in which states are a totally ordered set, and therefore, all relations have to be evaluated.

High computational requirements are also the case of the general framework for planning with uncertainty based on the partially observable Markov decision process (POMDP) [5]. On the other hand, sampling based techniques based on an extension of the configuration space by an "uncertainty dimension" seem to provide computationally feasible solution [6]. However, the key issue is an efficient determination of the collision probability with position uncertainty [7].

An alternative to the belief space planning approach has been presented in [8], where Belief Roadmap (BRM) approach is proposed. The BRM is a variant of the Probabilistic Roadmap algorithm for linear Gaussian systems, where nodes of the graph built have associated information about belief estimation. Thus, the roadmap allows to plan a trajectory regarding its length and uncertainty along it.

The aforementioned planning approaches consider uncertainty in sensors' measurements or in a robot position estimation using a regular localization function, e.g., based on the update step of the EKF. In the proposed approach, we rather consider a model of the localization uncertainty evolution based on a mathematical formulation of the navigational method [10]. The main advantage of the proposed approach is an efficient determination of the robot position uncertainty along a path consisting of a sequence of straight line segments. The basic formula describing the position uncertainty is a simple matrix equation that allows us to consider the path planning problem as an instance of the multi-goal path planning problem (MTP). The MTP is formulated as the well-know Traveling Salesman Problem (TSP) [11], [9], which is known to be NP-hard. The TSP stands to find a best sequence of goals visits; however, an order of goals' visits affects the precision of the goals' visits. Thus, we propose a planning framework for the MTP with the localization uncertainty. Although the graph based TSP solver can be eventually used with the BRM, the framework proposed does not require explicit construction of a graph before solving the TSP; thus, a solution found does not depend on sampling strategy as PRM based approaches.

We introduced the initial idea of the framework in [12],

Authors are with the dept. of Cybernetics, Faculty of Electrical Engineering, Czech Technical University in Prague, Technická 2, 166 27 Prague, Czech Republic {xfaigl}@labe.felk.cvut.cz

where the Parrot AR.Drone has been utilized in the verification of the main principle of the proposed MTP solver. The real experimental results show that the proposed planning improves the success rate of the goals' visits from 82.5 % to 95 %. However, this initial work is rather limited, and therefore, in this paper, we extend the framework to deal with environments with obstacles. Moreover, we generalize the model of the autonomous navigation to consider local properties of the environment and develop local models of visible landmarks used for the navigation. The generalized framework and its experimental verification in real outdoor environment are the main contribution of this paper.

The paper is organized as follows. The problem addressed is specified in the next section. In Section III, the main idea of the localization uncertainty decreasing is presented. The proposed MTP framework is described in Section IV. The experimental results are presented in Section V, and concluding remarks are dedicated to Section VI.

II. Problem Statement

The problem addressed is an instance of the inspection path planning for a mobile robot operating in a planar environment. The map of the environment is a priori known, and it is represented as a polygon with holes $\mathcal{W}$. Obstacles of $\mathcal{W}$ are enlarged to respect dimensions of the robot and the required clearance. It is assumed the robot has differential drive; thus, a point robot model is considered in $\mathcal{W}$. A set of n goals $\boldsymbol{G} = \{g_1, \ldots, g_n\}$ representing areas of interest to be visited is given, and each goal $g \in \boldsymbol{G}$ is reachable by the mobile robot, $g \in \mathcal{W}$. The considered multi-goal path planning problem is as follows: *Find a closed shortest path in $\mathcal{W}$ visiting all goals of $\boldsymbol{G}$ while the localization error of the robot at the goals is minimized.* Without loss of generality the starting point is assumed to be $g_n \in \boldsymbol{G}$.

The problem addressed is a variant of the well-known Traveling Salesman Problem (TSP), in which not only the path length is considered, but also the localization error is taken into account. As two criteria are minimized, it is clear that only Pareto optimality can be achieved. The problem is how the length of the path and the localization uncertainty at the goals relate, and what improvements can be achieved.

A. Models of the Localization Uncertainty

An efficient and informative heuristic function is needed to incorporate the localization uncertainty into the path planning algorithm. We assume that the mobile robot performing the inspection is navigated by the method presented in [10], where a proof of stability of the method and its experimental validation can be found. The method uses a map of salient objects of the environment, and matches the current seen objects to steer the robot in the desired direction. Assuming distance and heading estimations are independent and not correlated (e.g., using odometry for distance measurement and vision based heading estimation), the position uncertainty can be expressed in terms of covariance matrices [10]. For a robot navigated along a straight line segment (with the length s_i) from the position a_i, the covariance matrix $\boldsymbol{A}_{i+1}$ at the end of the segment i (position a_{i+1}) can be computed using the formula[1]:

$$\boldsymbol{A}_{i+1} = \boldsymbol{R}_i^T \boldsymbol{M}_i \boldsymbol{R}_i \boldsymbol{A}_i \boldsymbol{R}_i^T \boldsymbol{M}_i^T \boldsymbol{R}_i + \boldsymbol{R}_i^T \boldsymbol{S}_i \boldsymbol{R}_i, \quad (1)$$

where

$$\boldsymbol{M}_i = \begin{bmatrix} 1 & 0 \\ 0 & m(a_i, a_{i+1}, \mathcal{M}) \end{bmatrix}, \boldsymbol{S}_i = \begin{bmatrix} s_i\eta^2 & 0 \\ 0 & \tau^2 \end{bmatrix},$$

$m(a_i, a_{i+1}, \mathcal{M})$ represents a model of visible landmarks used for the navigation, $\boldsymbol{R}$ is the rotation matrix, and η, τ represent precision of the odometry and the heading sensor, respectively.

1) Global model of visible landmarks: For homogeneously distributed landmarks the model can be characterized using a single parameter ρ representing an "average" distance of the landmarks ahead of the robot. In this case, the function m can be expressed as [10]:

$$m(a_i, a_{i+1}, \mathcal{M}) = e^{-\frac{s_i}{\rho}}. \quad (2)$$

2) Local model of visible landmarks: Alternatively a map of the landmarks $\mathcal{M}$ can be utilized to compute expected distance of the closest landmark to the robot traveling from the position a_i towards the position a_{i+1}. Let the distance of such a landmark be d. Then, the model can have a form:

$$m(a_i, a_{i+1}, \mathcal{M}) = \frac{d}{s_i + d}, \quad (3)$$

which describes position of the robot moving towards a particular landmark. A particular value of d can be computed using various approaches depending on the representation of $\mathcal{M}$, e.g., point or polygonal map of landmarks. An expected benefit of the local model is a more precise estimation of the localization uncertainty; however, it is clear that it can be more computationally demanding than the global model.

B. Solution Quality Metrics

A natural quality metric of the inspection path visiting the given goals is a length of the path L. However, a robot can miss the goal due to imprecise navigation. Hence, an additional quality metric can be the maximal expected localization uncertainty at the goals. Using the navigational method [10], the uncertainty can be described by Eq. 1, and the expected position error at a goal g can be computed using the maximal eigenvalue of the matrix $\boldsymbol{A}_g$. Thus, the maximal localization error is

$$E_{max} = \max_{g \in \boldsymbol{G}} \sqrt{(||\boldsymbol{A}_g||^2)}. \quad (4)$$

Beside the quality metrics L and E_{max} of an inspection path found, the real performance of the autonomous inspection can be measured by real distances of the robot to the goals, when the robot announces that it reaches the particular goal. The real distances are examined in the experimental evaluation of the proposed planning method in Section V.

[1]Here, it is worth to mention that s_i in $\boldsymbol{S}_i$ is not in power of two, which is accidentally presented in [10].

III. Principle of Uncertainty Decreasing

A principle of the uncertainty decreasing utilized in the proposed multi-goal path planning is based on a geometrical interpretation of Eq. 1. The idea is as follows. Assume a robot moving from a goal g_1 to a goal g_2 along a straight line segment. The error in the longitudinal direction caused by the odometry is increased, while the error in the lateral direction is decreased due to heading corrections, see Fig. 1a where the corresponding covariance matrices $\boldsymbol{A_1}$ and $\boldsymbol{A_2}$ are visualized as ellipses [13]. In Fig. 1b, it is shown how the error can be decreased by an auxiliary navigation waypoint placed at a selected perimeter around g_2.

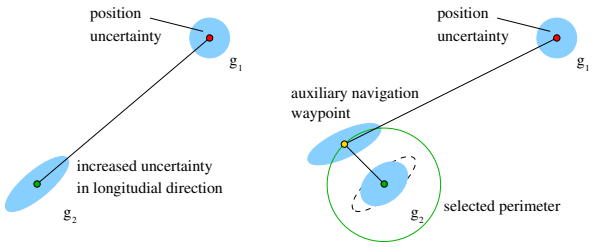

(a) direct connection of goals (b) auxiliary navigation waypoint

Fig. 1: A principle of the localization uncertainty decreasing.

This principle motivates us to consider visitation of an auxiliary navigation waypoint prior each goal visit. The auxiliary waypoint should be placed at a location that will suppress the error in a direction corresponding to the eigenvector of the maximal eigenvalue of the matrix $\boldsymbol{A}_i$. However, due to non-linearity of Eq. 1, such a location is not easy to compute. Moreover, the location can be unreachable due to obstacles. Therefore, eventual auxiliary waypoints are spread around each goal, and an appropriate waypoint is determined during the multi-goal path planning.

IV. Multi-Goal Path Planning with Localization Uncertainty

Herein, we extend the approach [12] to problems with obstacles using the algorithm [14]. The planning algorithm proposed is a type of unsupervised learning procedure that is a two-layered competitive learning network. An input vector i represents coordinates (g_{i1}, g_{i2}) of the goal g_i, and m output units form the output layer where neurons' weights (ν_{j1}, ν_{j2}) of the node ν_j are points in $\mathcal{W}$. The output units are organized into a unidimensional structure that prescribes a sequence of nodes representing a path in $\mathcal{W}$ in which the first node ν_1 and the last node ν_m denote the orientation of the path. For each goal g a set of auxiliary navigation waypoints is created, e.g., using a perimeter with radius d_p like in [12], but in this case only points inside $\mathcal{W}$ are associated to the goal, $P_g = \{p_{g,i} | p_{g,i} \in \mathcal{W}\}$.

During the learning, the goals are presented to the network in a random order, and for each goal a winning neuron is found using the length of approximate shortest path in $\mathcal{W}$ [14]. To ensure a path will be closed at the desired final goal g_n, the end nodes (ν_1 and ν_m) are adapted to g_n without competition. The node ν_1 and its neighbouring nodes ν_j (for $j > 1$) are adapted by a regular adaptation to g_n, while ν_m and its neighbouring nodes are adapted by the double adaptation rule, called *dadapt*.

The *dadapt* rule adapts nodes to the presented goal and a particular auxiliary navigation waypoint. Each node has associated the localization uncertainty represented by the covariance matrix A_ν. The matrix A_{ν_i} is computed from $A_{\nu_{i-1}}$ by Eq. 1, where a path among obstacles between two nodes is considered, i.e., the path between the nodes is a sequence of straight line segments; thus, each segment of the path is considered using Eq. 1. The matrix A_{ν_1} is computed from the approximate path from g_n to the node because ν_1 can be far from g_n during the adaptation. The initial uncertainty for g_n is set to zero. For a winner node $\nu^\star$ of the goal g, the *dadapt* rule is performed as follows. The backward neighbouring nodes of $\nu^\star$ are adapted to the perimeter point $p_{g,\star}$, while $\nu^\star$ and its forward neighbouring nodes are adapted to g. A point $p_{g,\star}$ is selected from the set P_g to minimize the dominant eigenvalue of $\boldsymbol{A}_g$. Because the adaptation changes positions of the nodes, the covariance matrices are recomputed prior each selection of the perimeter point.

An example of the network evolution is shown in Fig. 2. In all presented figures in this paper, the error ellipses are four times enlarged to show the effect of the uncertainty decreasing.

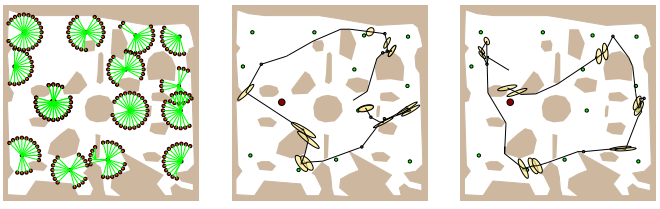

(a) perimeter points (b) step 3 (c) step 10

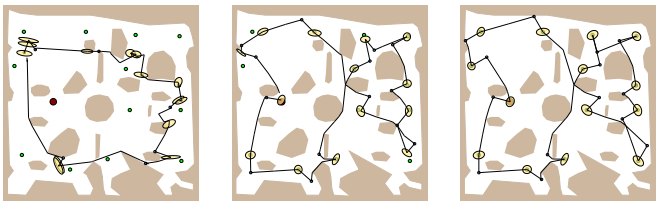

(d) step 22 (e) step 45 (f) step 64

Fig. 2: An example of the path evolution, the green disks represent goals, blue disks are nodes associated to the auxiliary navigation waypoints, the error ellipses are drawn for the winner nodes. The starting point (g_n) is shown as the brown disk.

The advantage of the propose algorithm is the ability to deal with obstacles while minimizing the both quality metrics. The obstacles cause that a path between two goals consists of several segments, which can eventually increase the precision of the navigation. However, the real benefit is not clear, and therefore, the performance of the real autonomous navigation using the proposed planning algorithm

is compared with a simple solution of the TSP (without localization uncertainty) in the experimental part of this paper.

A. Placement of Auxiliary Waypoints

In [12], we place auxiliary waypoints at a selected perimeter and an influence of perimeter radius to the solution quality has been shown. Also in the presence of obstacles, the radius affects the solution quality. Although an appropriate radius can be found experimentally (i.e., solving the problem individually for selected perimeters several times), the flexibility of the underlying self-organizing map algorithm allows to consider a general set of waypoints at various perimeters.

B. Local Models of Visible Landmarks

Eq. 3 pre-scribes how visible landmarks affect the localization uncertainty. A practical implementation of the formula can be based on a polygonal map of the visible landmarks or point landmarks can be directly used. In the first case, visible objects form obstacles and the distance d to the closest visible landmark can be found using an intersection of the supporting line of the path's segment with a segment forming the polygonal representation of the landmarks $\mathcal{M}_{polyg}$. An example of the superimposed landmark map is shown in Fig. 3, the map has been created from the ortophotomap shown in Fig. 4. Thus, the obstacles in this landmark map represent objects, where eventual landmarks can be seen.

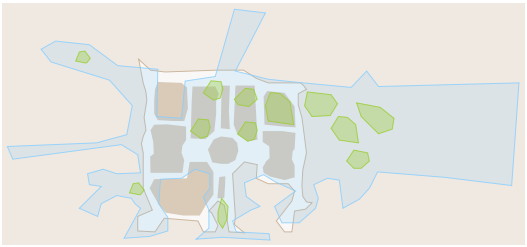

Fig. 3: An example of the polygonal map representing landmarks; the blue polygon is a boundary polygon of the surrounding area and the green polygons represents visible objects within the experimental site, e.g., trees.

Alternatively, landmarks can be represented by a set of points. In this case, it is necessary to consider a field of view (FoV) of the forward looking camera used for the navigation because a point landmark will not likely be placed exactly at the supporting line. An example of such a model is visualized in Fig. 6.

Similarly, the FoV can be considered also for $\mathcal{M}_{polyg}$. Assume a path segment (a_i, a_{i+1}), then the expected landmark is found as an intersection point p of a half-line started at a_{i+1} with a segment of $\mathcal{M}_{polyg}$. Such a point p must also be within the FoV defined by the segment (a_i, a_{i+1}), which provides a rough approximation of the expected landmark. The distance d in (3) is computed as $d = ||(a_i, p)||$. Moreover, this model allows additional visibility constraints, e.g., distance constraints regarding a texture of the objects.

It may happened that an expected landmark is not found by the proposed models due to local properties of the environment model $\mathcal{M}$ around the position a_i. In such a case, the function m has value 1, which corresponds to a landmark placed at infinity, regarding (2).

C. Computational requirements

The complexity of the proposed planning algorithm is proportional to the square of the number of goals multiplied by a number of navigational waypoints associated to one goal. The solutions presented in this paper are typically found in tens of milliseconds for waypoints on a single perimeter and in hundreds of milliseconds for several perimeters using C++ implementation and 3 GHz single core workstation.

V. Experiments

The idea of the uncertainty decreasing presented in Section III has been examined in real experiments with two types of robots, see Fig. 4b and Fig. 4d. All robots have been navigated using the method [10]. First, the benefit of the proposed planning method in real environment with obstacles (a city park) has been examined. Then, the effect of the local models has been examined in a simple scenario using four goals.

In all experiments, the parameters of the navigational model have been estimated for the particular robot and environment. Two paths visiting the given set of goals are used in each experimental scenario. The first path is a solution of the TSP without localization uncertainty denoted as *simple*. The second path is found using the proposed algorithm that is denoted as *dadapt*. For each method, the robot is taught the found path first. Then, the robot is requested to traverse the path several times while its position to the particular goal has been measured whensoever the robot announced it reached the goal. Supplementary materials describing the experiments can be found in [15].

A. Scenario 1 - Autonomous Navigation in a City Park

The P3AT mobile robot has been used to verify the proposed method in a real outdoor experiment in which five goals have been placed within the Charles Square location, see Fig. 4. For each algorithm variant twenty solutions have been found for parameters ρ=15, τ=0.001, ϵ=0.05, d_p=5 m, and a polygonal map created on top of the park orthophotomap. Impassable terrain has been marked as obstacles, which have been enlarged by a small distance to reflect the robot's dimensions and its possible localization error. The best found paths (regarding E_{max}) are depicted in Fig. 5. After the planning, the robot position at the goals' locations has been marked on the ground by a chalk during the path learning. Then, the robot has been requested to traverse the path autonomously for five times. Average robot distances to the goals are presented in Table I. The sample variances of the distances are 0.37 m and 0.32 m for the *simple* and *dadapt* methods respectively.

In this experimental scenario, the robot autonomously traveled about two kilometers. Although the path is found

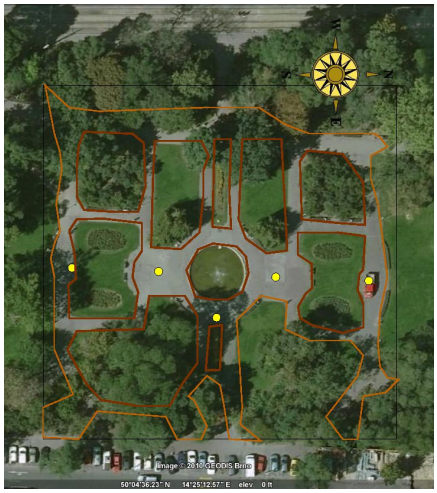

(a) a map of the Charles Square park in Prague, the goals are represented by small yellow disks

(b) the P3AT mobile robot during experiment

(c) indoor testing site

(d) MMP-5 platform

Fig. 4: The outdoor and indoor experimental sites.

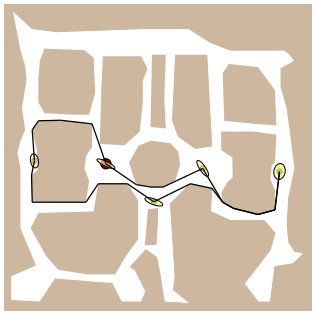

(a) *simple*, L=184 m, E_{avg}=0.57, E_{max}=0.63

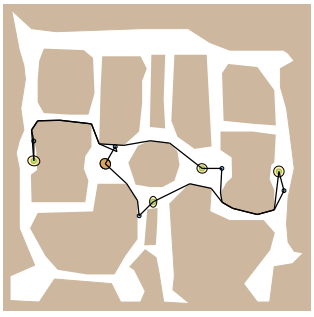

(b) *dadapt*, L=202 m, E_{avg}=0.35, E_{max}=0.37

Fig. 5: Best solutions found for the Charles Square scenario, d_p=5 m, and the global landmarks model.

TABLE I: Real P3AT distances to the goals

Planning method	**Average distances to the goals** [m]					
	g_1	g_2	g_3	g_4	g_5	overall
simple	0.71	0.92	0.94	0.97	0.93	0.89
dadapt	0.33	0.61	0.71	0.55	0.70	0.58

regarding the dimensions of the robot (using the Minkowski sum), the robot leaved the pathway occasionally due to imprecise localization. These errors do not cause a collision with obstacles, as far landmarks are used for the navigation, and a grass terrain is mostly around the pathways. The robot has been manually moved to the pathway only once and just its lateral position has been changed, i.e., the navigation has been paused, the robot has been moved, and requested to continue the navigation without any additional settings. In this particular case, the robot has been completely on the grass, in other cases at least one wheel remains on the pathway.

B. Scenario 2 - Small Low-Cost Wheeled Mobile Robot

The second experiment has been performed in an indoor environment without obstacles with a MMP5 platform shown in Fig. 4d. A single camera is used for the navigation with the on-board processing using the NVidia ION platform. The identified parameters of the navigational model are ρ=7, η=0.05, and τ=0.01 meters. The goals form a rectangle with 3.750 $\times$ 4.375 m and the proposed *dadapt* method provides the same best paths regarding the lowest E_{max} over several runs and selected perimeters regardless models of landmarks described in Section IV. However, the expected values of E_{max} are different for different landmarks models, and generally the local models provide lower values than the global model. The best found path is visualized in Fig. 6. Real average distances of the robot positions from the goals computed over 10 runs of autonomous navigation are presented in Table II.

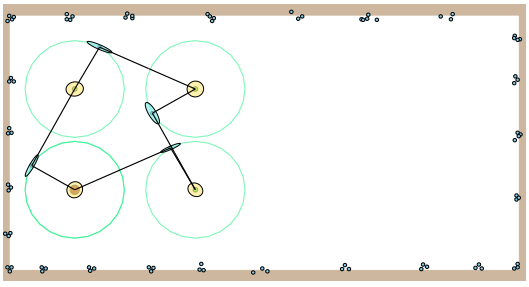

Fig. 6: The best path found using point based local model of landmarks. The blue disks represent landmarks.

TABLE II: Real MM5 distances to the goals

Planning method	**Average distance to the goal** [cm]				
	g_1	g_2	g_3	g_4	overall
simple	12.9	14.3	20.4	18.7	16.6
dadapt	9.7	12.6	12.8	16.2	12.8

The expected ratio of the localization uncertainty decrease is about 0.7 using E_{max} for the paths found by the *single* and *dadapt* methods, while the achieved ratio is 0.8. The real average localization errors are 24.8 cm and 20.2 cm for the *single* and *dadapt* paths, respectively, and the maximal errors over all goals and runs are 34 cm and 27 cm, respectively. The cost of the uncertainty decrease is a bit longer path, which is approximately proportional to the uncertainty decrease, i.e., the length ratio is about 1.3.

C. Discussion

Although the expected uncertainty decrease (ratio of the E_{max} for the *single* and *dadapt* methods) differs from the real achieved ratio, the experimental results confirms the benefit of the planning method providing a path leading to a more precise visitations of the goals (about 20 %). The results show that even in the environment with obstacles, the proposed planning is beneficial.

The differences between the expected and achieved results are caused by several factors. First, all the parameters are only estimated. In addition, the global model is only a rough estimation providing average expected results, which in part holds also for the local models. Besides, it's clear that the real robot path cannot be exactly the planned path, unless precise (that means expensive and unpractical) navigation is used for learning the path. Despite that the planned paths provide real valuable guideline suggesting an order of the goals visits and the navigation waypoints.

On the other hand, the proposed generalizations of the planning method considering more auxiliary waypoints and local models of the landmarks do not provide significant benefit in a comparison with a single selected perimeter and the global model. This is mainly due to considered scenarios, which are rather simple. However, these generalizations form fundamental extensions towards a planning framework allowing to consider local properties of the environment and specific sensing device used for the navigation. It is expected that a proper local model will provide a more precise estimation of E_{max}, which will be closer to the really achieved error, as a more sophisticated model can be proposed. For example in the current local model, the expected visible landmark for a segment of the path is found using the segment end. It is assumed that such a landmark will be visible during the traversing the segment. The robot is navigated towards the landmark, and therefore, its distance to the landmark is decreasing. It is obvious that for a very long segment, this approximation is only rough, and a more sophisticated local models can be proposed, e.g., considering the fact that, in reality, closer landmarks along the segment are often used for the navigation. In addition, the eigenvalue used for E_{max} is not exactly the distance measured in real experiments.

VI. Conclusion

An extension of the multi-goal path planning with localization uncertainty for environments with obstacles has been presented. Moreover, generalization of our previous work to deal with a local model of landmarks has been introduced. The planning algorithm can use more navigational waypoints at different perimeters allowing to automatically find the best perimeter waypoint individually for each goal. The proposed approaches have been experimentally verified in real outdoor and indoor scenarios. Although the expected characteristics of the navigation for the planned path differ from the real performance, the benefit of the approaches to uncertainty decrease is evident from the results. All together, the generalized approach presented forms a suitable framework (with low computational requirements) for a further research in path planning with focus on surveillance tasks.

Our future aim is to improve the model of landmarks to achieve closer expected and real performance characteristics of the autonomous navigation to provide more realistic expectations.

Acknowledgments

This work has been supported by the Ministry of Education of the Czech Republic under Projects No. LH11053 and No. 7E08006, and by the EU Project No. 216342.

References

[1] H. Takeda, C. Facchinetti, and J.-C. Latombe, "Planning the motions of a mobile robot in a sensory uncertainty field," *IEEE Trans. Pattern Anal. Mach. Intell.*, vol. 16, pp. 1002–1017, October 1994.

[2] Y. Oshman and P. Davidson, "Optimization of observer trajectories for bearings-only target localization," *Aerospace and Electronic Systems, IEEE Transactions on*, vol. 35, no. 3, pp. 892 –902, July 1999.

[3] A. Lambert and D. Gruyer, "Safe path planning in an uncertain-configuration space," in *IEEE Int. Conf. Robotics and Automation (ICRA)*, vol. 3, sep. 2003, pp. 4185–4190.

[4] A. Censi, D. Calisi, A. D. Luca, and G. Oriolo, "A Bayesian framework for optimal motion planning with uncertainty," in *IEEE Int. Conf. on Robotics and Automation (ICRA)*, Pasadena, CA, May 2008.

[5] L. P. Kaelbling, M. L. Littman, and A. R. Cassandra, "Planning and acting in partially observable stochastic domains," *Artif. Intell.*, vol. 101, pp. 99–134, May 1998.

[6] R. Pepy, M. Kieffer, and E. Walter, "Reliable robust path planning with application to mobile robots," *Int. J. Appl. Math. Comput. Sci.*, vol. 19, no. 3, pp. 413–424, 2009.

[7] Y. Huang and K. Gupta, "Collision-probability constrained prm for a manipulator with base pose uncertainty," in *IEEE/RSJ Int. Conf. Intelligent Robots and Systems (IROS)*, 2009, pp. 1426 –1432.

[8] S. Prentice and N. Roy, "The belief roadmap: Efficient planning in belief space by factoring the covariance," *Int. J. Rob. Res.*, vol. 28, pp. 1448–1465, November 2009.

[9] M. Saha, T. Roughgarden, J.-C. Latombe, and G. Sánchez-Ante, "Planning Tours of Robotic Arms among Partitioned Goals," *Int. J. Rob. Res.*, vol. 25, no. 3, pp. 207–223, 2006.

[10] T. Krajník, J. Faigl, V. Vonásek, K. Košnar, M. Kulich, and L. Přeučil, "Simple yet stable bearing-only navigation," *Journal of Field Robotics*, vol. 27, no. 5, pp. 511–533, 2010.

[11] S. N. Spitz and A. A. G. Requicha, "Multiple-Goals Path Planning for Coordinate Measuring Machines," in *IEEE Int. Conf. on Robotics and Automation (ICRA)*, 2000, pp. 2322–2327.

[12] J. Faigl, T. Krajník, V. Vonásek, and L. Přeučil, "Surveillance planning with localization uncertainty for mobile robots," in *Proceeding of the 3rd Israeli Conference on Robotics*, 2010.

[13] R. Smith and P. Cheeseman, "On the representation and estimation of spatial uncertainty," *International Journal of Robotics Research*, vol. 5, no. 4, pp. 56–68, 1986.

[14] J. Faigl, M. Kulich, V. Vonásek, and L. Přeučil, "An Application of Self-Organizing Map in the non-Euclidean Traveling Salesman Problem," *Neurocomputing*, vol. 74, no. 5, pp. 671–679, 2011.

[15] "On localization uncertainty in an autonomous inspection with bearing-only navigation," videos from experiments and supplementary material, http://purl.org/faigl/planning.